COMMUNICATION

ChemComm
www.rsc.org/chemcomm

Cruciform π-systems: effect of aggregation on emission†

James N. Wilson,[a] Mark D. Smith,[b] Volker Enkelmann[c] and Uwe H. F. Bunz*[a]

[a] *School of Chemistry and Biochemistry, Georgia Institute of Technology, 770 State St, Atlanta GA 30332, USA. E-mail: uwe.bunz@chemistry.gatech.edu; Fax: +1 404 385 1795; Tel: +1 404 385 1795*

[b] *Department of Chemistry and Biochemistry, University of South Carolina, Columbia SC 29908, USA*

[c] *Max-Planck Institut für Polymerforschung, D-55021 Mainz Postfach 3148, FRG*

Received (in Columbia, MO, USA) 16th April 2004, Accepted 25th May 2004
First published as an Advance Article on the web 28th June 2004

The solid state properties of cruciform pentamers 1–4 are examined in thin film preparation, in the single crystalline state and in nanoparticle formulations; emission behavior was found to vary substantially with the solid state morphology. This type of behaviour is an excellent way to manipulate the emissive properties of conjugated π-systems.

Conjugated organic oligomers have been used extensively in optical and electronic devices.[1] We recently introduced a class of cross-conjugated oligomers **1–4** that show unusual electronic properties in solution.[2,3] To achieve successful incorporation of these and other conjugated materials into functional solid state devices it is necessary to understand and manipulate their solid state optical properties as a consequence of their intermolecular ordering[4] and their conformational preference.[5] We find that the morphology, *i.e.* crystalline or glassy state[6] of these molecules, has a substantial effect upon their emission spectra, similar to the oligomers extensively examined by Curtis *et al.*[4]

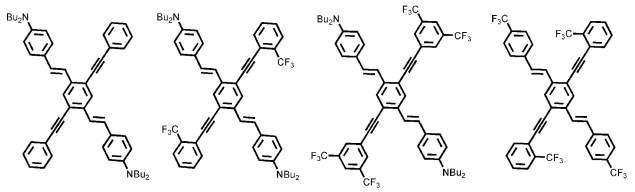

Scheme 1

While spun cast films of **1–4** were found to be amorphous, crystallization of **1–4** from a mixture of dichloromethane and methanol (**1–3**) or from xylenes (**4**) resulted in specimens suitable for single crystal XRD (Fig. 1). The most striking characteristic of these structures is the relative distortion of the π-system. While **3** exhibits near perfect planarity of the π-backbone, **1** and **2** show twisting of the phenyleneethynylene (PE) subunits with rotations of approximately 30°. Additionally, the styryl groups of **2** show a departure from planarity. Twisting of approximately 15° of the PE unit in **4** is observed. While **2** and **3** pack in a herringbone fashion, **1** exhibits flat packing. In **2** the electron poor, CF_3-substituted arenes are in an edge-on contact to the electron rich NBu_2-substituted benzene rings. No other secondary interactions of electron rich to electron poor arenes were detected, however, in the packing of **1–4**. To examine the solid state optical spectra of **1–4**, thin films were cast from chloroform solution. The films were amorphous when examined under the crossed polarizers of an optical microscope. As expected, the molecules **1–3** showed similar absorption spectra (thin films, see Table 1) with a first maximum between 330 and 340 nm and a second, broader maximum between 425 and 455 nm. Only one emission peak is observed in thin films of **1–3** ranging from 560 to 586 nm respectively. An absorption maximum of 332 nm and an emission maximum of 484 nm were observed for **4**, substantially blue shifted from its dibutylamino-substituted relatives **1–3**.

† Electronic supplementary information (ESI) available: X-ray data of **1–4** and electron diffraction (experimental and simulated) of **3**. See http://www.rsc.org/suppdata/cc/b4/b406495j/

We next examined the emission of crystals of **1–4** (Table 1). A similar trend was observed as in the thin films with **4** showing the bluest emission at 504 nm, **1** and **2** displaying emissions near 600 nm while **3** was again the reddest at 607 nm. For **4** this represents a 20 nm shift from the thin film, while for **3** the shift is 21 nm and in **1** a 40 nm shift is observed. It was of interest to see whether these crystals could be converted to the glass-like state to compare the resulting emission spectra with those observed in the crystalline state. None of the compounds formed the desired glassy state with the exception of **1** which could easily be drawn into amorphous fibers that were up to 10 cm in length with widths of ~100 μm. Powder XRD (Fig 2, top left) shows the effect of melting on **1**: a distinct diffraction pattern is visible before and an amorphous pattern is visible after melting. This loss of crystallinity corresponds to a 25 nm red shift in emission confirming the observed difference between thin film and crystal. By comparison, **4** shows a quite different behavior—attempts at melting the sample resulted

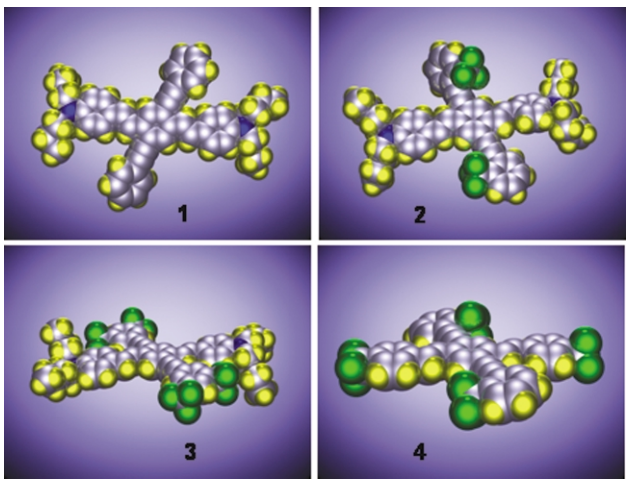

Fig. 1 Crystal structures of compounds **1–4** showing the twist angles of the phenyleneethynylene subunits in **1** and **2** (30° and 45° respectively), while **3** and **4** (12°) remain relatively planar.‡

Table 1 Summary of the optical and crystal data for **1–4**

	1	**2**	**3**	**4**
Absorption, film/nm	335, 440	340, 455	335, 425	332
Emission, film/nm	560	574	586	484
Emission, crystal/nm	601	596	607	504
Emission, solution/nm	498 (C_6H_{14})	502 (C_6H_{14})	579 (THF)	434 ($CHCl_3$)
Space group	$P2_1/c$	$P2_1/n$	$C2/c$	$P2/c$
a	14.78 19.60	13.83	42.33 5.19	17.87 5.06
b	16.74	16.94	28.82	18.69
c		20.42		
β/°	115.63	97.85	128.21	97.6
Z	4	4	4	2

DOI: 10.1039/b406495j

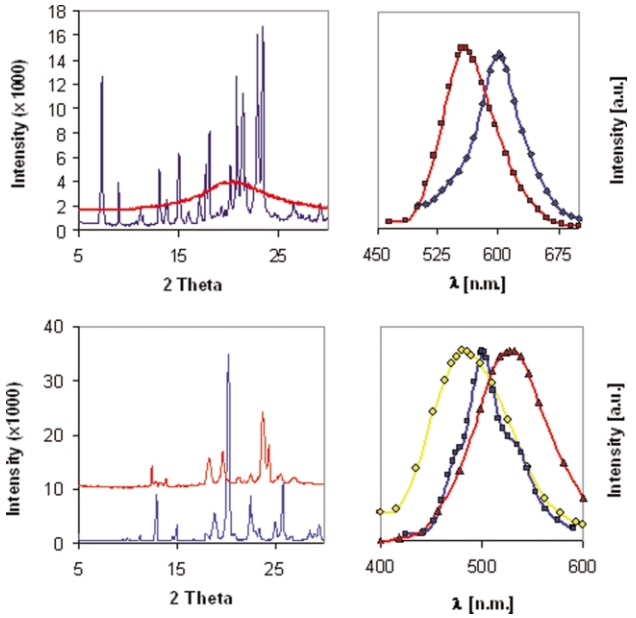

Fig. 2 Compound **1** (top) shows a distinct XRD pattern for the crystalline state and emission at 601 nm (blue). Melting and cooling the sample results in loss of crystallinity (red) and a hypsochromic shift of 25 nm in the emission. Crystals of **4** (at bottom) display a distinct XRD pattern and an emission centered at 504 nm (blue). Melting and cooling this sample results in a second crystalline state with 25 nm red shifted emission (red). Amorphous thin films display an emission (yellow) at 484 nm.

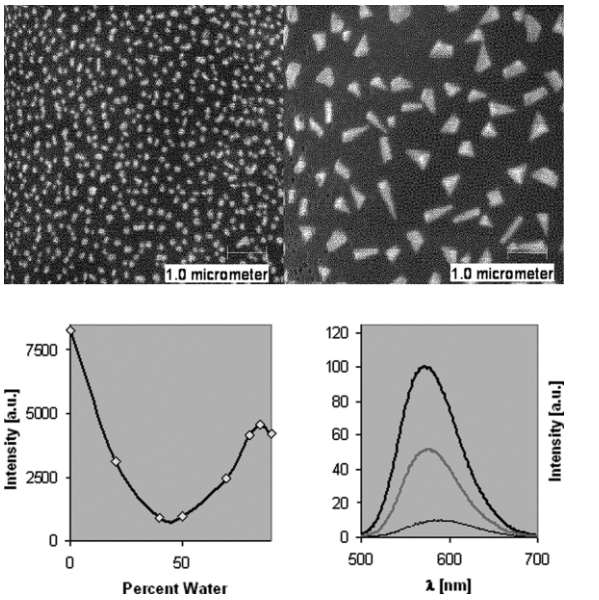

Fig. 3 Nanospheres of **1** (top left) and nanocrystals of **3** (top right) with scale bar. Nanoparticles are formed by the addition of water to THF solutions of the compounds. Bottom left: relative quantum yield of **3** as a function of H_2O–THF fraction. Quantum yield of **3** in THF Φ = 0.10. Bottom right: With initial addition of H_2O the quantum yield drops (thin line), but increases at higher H_2O concentrations (grey line).

in another crystalline state as observed in the XRD pattern (Fig 2, bottom left). The emission spectra of this second crystalline state was found to have its emission *red* shifted by 20 nm. Thus **4** exhibits three solid state emissions (Fig 2, bottom right) (a) amorphous thin films yielding the bluest emission at 484 nm, (b) one crystalline state emitting at 504 nm and (c) a second crystalline state emitting at 526 nm.

Preparations of nanospheres from conjugated oligomers and polymers have been reported, the simplest method being that reported by Park *et al.*[7] Nanospheres have been successfully incorporated into functional solar cells.[8] It was of interest to see if **1–4** could form nanospheres from THF–H_2O mixtures and in how far their optical properties would be different from that of thin film and crystalline preparations. Dilute solutions (2.0×10^{-5} M) of **1–4** in THF with increasing fractions of water were prepared. The effect of water could be observed as a decrease in the quantum yield and a red shift (15 nm for **3**, Fig. 3, bottom) in emission. However, above ~75% H_2O concentration, the emission of **3**, but not that of **1, 2**, or **4**, showed a dramatic *increase* in intensity accompanied by a small hypsochromic shift. We believe this behavior results from the formation of the nanoparticles: molecules of **3** are isolated from their polar environment (THF–H_2O mixture) and thus exhibit a higher quantum yield and slight blue shift. The behavior is not observed in the nanoparticle preparation of the other cruciforms.

SEM images revealed that **1** showed nanospheres of uniform size and shape (150–250 nm, Fig. 3, top left) similar to those previously reported,[7] while **3** formed well-developed nanocrystals (widths of 200–500 nm, lengths of up to 1 μm, Fig 3, top). While electron diffraction patterns were observed for **3**, the microspheres of **1** were amorphous. Electron diffraction showed that the nanocrystals of **3** exhibited the same packing as that observed in macroscopic single crystals according to comparison of the actual electron diffraction pattern to a simulated one obtained by the program Cerius[2] (ESI†) utilizing the cell data obtained from macroscopic single crystals of **3**.

Cruciforms **1–4** form distinctly different morphologies in the solid state (thin film, crystalline phases, nanoparticles) displaying greatly different emissive behavior. It is to be noted that while **1,2** and **4** form nanospheres, **3** forms highly fluorescent nanocrystals. In the future we will report on the incorporation of these nanomaterials into LEDs and thin film transistors.

We thank DARPA and NSF (DMR 0138948) for generous funding.

Notes and references

‡ Compound **1**: $C_{54}H_{60}N_2$, M = 737.04, monoclinic, a = 14.7777(7), b = 19.5961(9), c = 16.7434(8) Å, β = 115.634(1)°, U = 4371.4(4) Å^3, T = 200.0(2) K, space group $P2_1/c$ (no. 14), Z = 4, μ(Mo–Kα) = 0.064 mm^{-1}, $R1$ and $wR2$ were 0.0541 and 0.1400 ($I > 2\sigma I$). **2**: $C_{56}H_{58}F_6N_2$, M = 873.04, monoclinic, a = 13.8368(7), b = 16.9399(8), c = 20.4197(10) Å, β = 97.8490(10)°, U = 4741.4(4) Å^3, T = 150.0(2) K, space group $P2_1/n$ (no. 14), Z = 4, μ(Mo–Kα) = 0.087 mm^{-1}, $R1$ and $wR2$ were 0.0596 and 0.1407 ($I > 2\sigma I$). **3**: $C_{58}H_{56}F_{12}N_2$, M = 1009.05, monoclinic, a = 42.330(2) Å, b = 5.1937(2) Å, c = 28.821(1) Å, β = 128.2140(10)°, U = 4978.4(3) Å^3, T = 150(1) K, space group $C2/c$ (no. 15), Z = 4, μ(Mo–Kα) = 0.109 mm^{-1}, $R1$ and $wR2$ were 0.0541 and 0.1423 ($I > 2\sigma I$). **4**: $C_{42}H_{22}F_{12}$, M = 754.60, monoclinic, a = 17.8688(14), b = 5.0625(4), c = 18.6933(18) Å, β = 97.617(2)°, U = 1676.1(2) Å^3, T = 150(1) K, space group $P2/c$ (no. 13), Z = 2, μ(Mo–Kα) = 0.133 mm^{-1}, $R1$ and $wR2$ were 0.0546 and 0.1344 ($I > 2\sigma I$). CCDC 218374–218377. See http://www.rsc.org/suppdata/cc/b4/b406495j/ for crystallographic data in .cif or other electronic format.

1 *Electronic Materials. The Oligomer Approach*, eds. K. Müllen and G. Wegner, Wiley-VCH, Weinheim, 1998.
2 J. N. Wilson, M. Josowicz, Y. Wang and U. H. F. Bunz, *Chem. Commun.*, 2003, 2962.
3 For other cruciform oligomers see: J. E. Klare, G. S. Tulevski, K. Sugo, A. de Picciotto, K. A. White and C. Nuckolls, *J. Am. Chem. Soc.*, 2003, **125**, 6030.
4 A. B. Koren, M. D. Curtis, A. H. Francis and J. W. Kampf, *J. Am. Chem. Soc.*, 2003, **125**, 5040–5050; A. B. Koren, M. D. Curtis and J. W. Kampf, *Chem. Mater.*, 2000, **12**, 1519.
5 C. E. Halkyard, M. E. Rampey, L. Kloppenburg, S. L. Studer-Martinez and U. H. F. Bunz, *Macromolecules*, 1998, **31**, 8655.
6 P. Strohriegl and J. V. Grazulevicius, *Adv. Mater.*, 2002, **14**, 1439.
7 B. K. An, S. K. Kwon, S. D. Jung and S. Y. Park, *J. Am. Chem. Soc.*, 2002, **124**, 14410.
8 T. Kietzke, D. Neher, K. Landfester, R. Montenegro, R. Guntner and U. Scherf, *Nat. Mater.*, 2003, **2**, 408.